ELSEVIER

Biochimica et Biophysica Acta 1411 (1999) 1–20

BIOCHIMICA ET BIOPHYSICA ACTA
BBA

Review

Femtosecond processes in proteins

Marten H. Vos *, Jean-Louis Martin

INSERM U451, Laboratoire d'Optique Appliquée, Ecole Polytechnique-ENSTA, 91761 Palaiseau Cedex, France

Received 17 November 1998; received in revised form 8 February 1999; accepted 11 February 1999

Keywords: Femtosecond spectroscopy; Nuclear dynamics; Vibrational coherence; Reaction center; Retinal protein; Heme protein

Contents

1. Introduction

The functioning of proteins relies on their capacity to efficiently adopt distinct spatial configurations

* Corresponding author. Fax: +33-1-6931-9996; E-mail: vos@enstay.ensta.fr

PII: S0005-2728(99)00035-3

upon interaction with highly specific entities from the environment. The purpose of the work that we review here is to get detailed insight in the internal dynamics underlying these specific configurational changes using a 'percussional' approach where the external trigger is close to a δ-function in time. The fastest structural changes taking place on the time scale of tens of femtoseconds (1 fs = 10^{-15} s), the external trigger synchronizing the time course of a biological reaction must be impulsive on this time scale. This requirement can only be met or approximated by using ultrashort optical pulses, both as impulsive perturbation and as a probe. Hence the interest in femtosecond spectroscopy in the elucidation of the fundamental mechanisms of biological processes. This technological restriction implies that only photoactivatable processes can be triggered and experimentally studied on the femtosecond time scale. However, general results from these studies may be extended to nonphotoactivatable processes.

Evidently, an eminent application of femtosecond spectroscopy is to study physiological light-driven processes, predominantly photosynthesis and vision, but also a variety of other processes, including phototaxis, light-induced DNA-repair, and green fluorescence. In addition, many proteins involved in other functions absorb light via colored cofactors (chromophores) and can thus be activated by a light pulse in the favorable situation where part of the absorbed photon energy is channeled to a reactive state. This is in particular the case for heme proteins, which are involved in a great variety of processes, including oxygen transport and storage (hemoglobin and myoglobin), local NO production (NO-synthase) and sensing (guanylyl cyclase), detoxification (cytochrome *P*450) and in particular in many respiratory and other bioenergetic functions (oxidases, cytochrome complexes). Furthermore, photoactivation via optically active artificial substrates bound to the protein may in principle gain insight into a variety of other biologically relevant processes.

On the femtosecond-to-picosecond time scale, intraprotein dynamics can be highly correlated. This property constitutes a fundamental difference with processes taking place on a longer time scale, where the dynamics are stochastic in nature. As a consequence, for ultrafast processes, concerted motions may play an important role in determining reaction efficiencies, and the thermodynamic concepts governing the slower processes are not necessarily applicable. The experimental demonstration of a regime of vibrational and, on a shorter time scale, electronic coherence, during ultrafast reactions is an important general achievement of femtosecond spectroscopic studies in the last decade.

We have previously reviewed 'femtosecond biology' in 1992 [1]. Since then, sub-50 fs solid-state femtosecond laser sources have become commercially available and the field has been rapidly expanding. Especially in combination with site-directed mutagenesis, femtosecond spectroscopy (in particular transient absorption) has become a widespread tool in structure–dynamics–function studies. In addition, during the last few years, the novel structure determination of several important photoactivatable proteins, including the B800–850 antenna complex [2], the Photosystem I reaction center [3], cytochrome *c* oxidase [4,5], green fluorescent protein [6,7], DNA-photolyase [8] and NO-synthase [9] have provided a structural basis for such studies. Recent developments in many of these domains have been treated in more specialized reviews. Without attempting to cover the entire literature, in the present time scale- and technique-oriented review we will focus on a few current issues involving the application of femtosecond spectroscopy, with an emphasis on the role of vibrational motion in ultrafast processes. The characteristics of the biological systems covered will be described only succinctly. We refer to more system-centered reviews for comprehensive introductions on these systems.

2. Experimental aspects

Very generally, ultrafast spectroscopic techniques are of the type pump-probe (Fig. 1). The photoprocess is synchronized by a relatively intense and necessarily short pump pulse. The spectroscopic response of the sample is probed by a weak probe pulse. The response time of conventional detection devices is too long to achieve femtosecond temporal resolution from a continuous probe source. Therefore, the probe pulse itself must also be short and its time-integrated characteristics (spectrum, intensity) are measured. A kinetic response is constructed

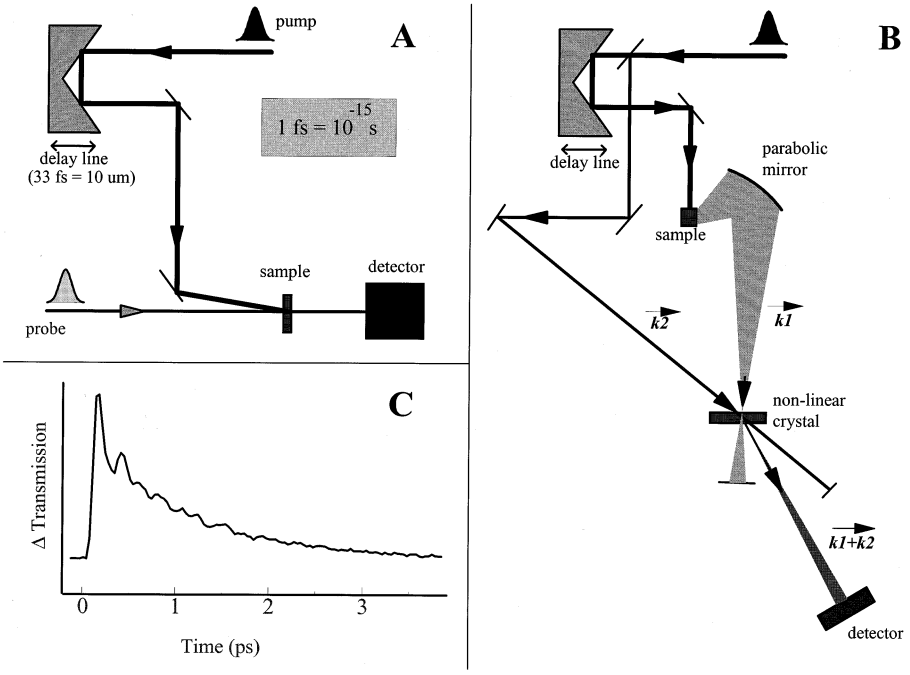

Fig. 1. Principle of femtosecond pump-probe spectroscopy. The time delay between pump and probe pulses is determined by the optical path length difference between the two pulses. (A) Scheme for transient absorption measurements. A probe pulse propagates through a volume of the sample illuminated by the pump pulse and its intensity or spectrum is monitored as a function of the delay time. (B) Scheme for transient emission measurements. The pump-pulse induced emission is gated by mixing with a reference pulse in a non-linear crystal and the upconverted fluorescence is detected at the sum-frequency of fluorescence and reference beam. (C) A kinetic trace is generated by varying the optical path of one of the pulses in a stepwise manner. The shown trace is a transmission kinetics of wild-type RCs from *R. sphaeroides* in the stimulated emission region [32]. It reflects both coherent nuclear dynamics in, and population decay of, the P* state.

by repeating the experiment at various values for the delay time between pump and probe pulse (Fig. 1C), equivalent to a sampling technique in electronics: 'sampling scope'. This is achieved by varying the relative optical path length of the pulse pair (in air, a path length difference of 10 μm corresponds to 33 fs). In different types of experiments, the repetition rate varies from ∼1 Hz to ∼100 MHz (oscillator frequency). Pulse lengths of 40–50 fs can now be obtained directly with commercially available oscillator/amplifier systems. However shorter pulses are routinely used in many laboratories and pulse lengths of less than 5 fs have been reported [10].

The main part of the experimental work reviewed here has been obtained with transient absorption spectroscopy, for which the general optical arrangement is displayed in Fig. 1A. Here, the transmission of a one-color or multicolor (white light) femtosecond probe pulse is recorded as a function of the delay time (Fig. 1C) and possibly, in the second case, the wavelength. Other commonly employed ultrafast optical techniques include transient Raman spectroscopy, photon echo spectroscopy and transient spontaneous emission (fluorescence) spectroscopy.

In transient Raman spectroscopy, the Raman scattering induced by the probe pulse is monitored. In this case, the temporal resolution is necessarily limited (typically to ∼1 ps) by the bandwidth requirement to ensure a reasonable spectral resolution. For biological applications, the technique has been applied almost exclusively to heme proteins. Following initial studies by Petrich and coworkers on the high-frequency ν_4 mode in hemoglobin [11], recent advances include the extension to the low-frequency (∼200 cm^{-1}) spectral region [12] and the improvement of the signal to noise ratio by the use of a kHz repetition rate solid-state laser, allowing to monitor reliably the anti-Stokes spectra [13].

In photon echo experiments, a transient grating

generated by two optical pulses is red out by an echo generated by a third pulse and emitted in a specific direction. This technique yields information about the electronic [14] and vibrational [15] dephasing, depending on the type of grating generated.

Finally, in spontaneous emission experiments, the sample interacts only with the excitation pulse, which populates an emitting electronic state. The fluorescence is focused into a nonlinear crystal and mixed with a probe pulse. The intensity of the generated pulse at the sum-frequency of the probe pulse and the fluorescence is then recorded as a function of the delay time between pump- and probe pulse (Fig. 1B). Using refractive optics to minimize frequency dispersion effects after the sample (they cannot be precompensated for), a time resolution of $\sim$130 fs has been obtained [16]. In addition to spontaneous emission, stimulated emission can be generated by probe light in resonance with the emitting transition. In a transient absorption arrangement this is manifested as light amplification in the direction of the beam; i.e., as a 'bleaching' of the sample, often in a spectral region where there is no ground state absorption [17].

To avoid jitter (spread in the timing of the probe pulse relative to the pump pulse), the pump and probe pulses are generally taken from, or derived from, the same laser source, a femtosecond solid state (titanium sapphire) or dye laser, operating in the visible or near-infrared (NIR). For many applications, the output of the oscillator is amplified at a lower repetition rate, using a (typically nanosecond) pulsed pump laser. In this way, light at a different spectral region can be generated using nonlinear processes such as frequency doubling, and self-phase modulation in the case of continuum generation. This light can subsequently be amplified, either by an external pump laser, as above, or parametrically, using the amplified femtosecond pulse as a pump. In most applications described here, a visible or NIR pump pulse is combined with a UV, visible, NIR or mid-infrared probe pulse. The latter can be obtained using difference frequency generation with two spectrally close-lying visible or NIR pulses, or alternatively by optical rectification in a semiconductor material of a spectrally broad and very short single pulse [18]. The latter technique also allows Fourier transform infrared (FTIR) spectroscopy with femtosecond resolution [19]; applications to biological systems have yet to be reported. More broadly, femtosecond electromagnetic pulses ranging from single cycle micrometer [18] to subnanometer X-ray [20,21] have been generated.

A few elements specific for femtosecond work are worth mentioning to understand specific requirements.

(1) Often, the technique operates near the bandwidth limit, that is near a regime where the temporal resolution corresponds to the spectral bandwidth of the pulses used. Hence the laser pulses used are far from monochromatic in the classical sense, even in so-called one-color experiments. For instance, for a pulse centered at 800 nm, a pulsewidth of 30 fs (full width at half maximum (fwhm)) corresponds to a spectral width of $\sim$22 nm (fwhm).

(2) Group velocity dispersion is an important parameter: any optically active material (lenses, windows, solvent, even air) through which the pulse propagates introduces dispersion (chirp) and hence pulse lengthening. To a certain extent these can be compensated for, but generally they are kept to a minimum, and for instance the group velocity dispersion effects impose a short (typically 1 mm or less) optical path length of the sample and a (near-)parallel arrangement of pump- and probe pulses.

3. Regimes of protein dynamics

As stated in the introduction, impulsive excitation of a system in a nonequilibrium nuclear configuration induces motions directed towards the (new) equilibrium conformation. The nature of these motions is relevant for understanding the mechanism of reactions taking place on the femtosecond time scale. A useful classical visualization of the possible regimes of these motions is the wave packet scheme (Fig. 2). Here a one-dimensional cross section of the potential energy surfaces of the ground state, excited state and possibly product electronic state is displayed along a – generalized – nuclear coordinate, with displaced potential energy minima. The protein multi-atom system has many intrinsic degrees of freedom and a corresponding dimensionality of the potential energy surfaces; yet the number of degrees of freedom for which the wells are significantly

displaced along a reactional pathway may be limited.

The absorption of a photon generates the excited state in an out-of-equilibrium configuration, the distribution of which is represented by a 'wave packet'. In the classical view of the Franck–Condon principle, the initial wave packet is the projection of the ground state thermal distribution, possibly weighted by the spectrum of the absorbed light. This packet initially evolves towards the equilibrium position. For the full dynamics of the wave packet, two regimes can be distinguished. First, the motions can be damped strongly by energy dissipation towards other degrees of freedom (friction), resulting in a rapid relaxation of the packet towards a thermal distribution, where the motion is stochastic (Fig. 2, upper panel). If, by contrast, frictional damping occurs on a time scale longer than the period corresponding to the curvature of the well, the wave packet will periodically move back and forth in a coherent fashion (Fig. 2, lower panel). This regime of motion in principle allows specific, external perturbation-selected motion of the protein, and exploration of configurations which are not thermally accessible.

In contrast to the stochastic regime, in the coherent regime, oscillatory beats associated with specific spectroscopic properties may be observed. This is illustrated in Fig. 2 for the case of probing emission from an impulsively populated excited state. This specific case is spectroscopically a relatively simple one as the same transition is used for excitation and probing [22]. However, other spectroscopic observables probing the excited state also can give rise to coherent kinetics [23], and furthermore coherent motion can be monitored on other potential energy surfaces, including that of the ground state, in which a wave packet can be created via the impulsive stimulated Raman effect [24] or via selective depopulation ('anti-wave packet') [25]. The latter effects are not directly relevant for biological functioning, but can be of high spectroscopic interest as a tool for studying the vibrational structure underlying absorption bands [26].

In almost all classical treatments of reaction dynamics, the ensemble of motions in the reactant state are assumed to be thermal. The observation, in the early nineties, of vibrational coherence in bacterial reaction centers [27] and subsequently in many other light-sensitive systems [28–31] has demonstrated that coherent motions contribute significantly to the dynamics of proteins on the picosecond time scale. This implies that the assumption of thermal equilibrium is not, or at least not generally, valid on this time scale.

In the following, we will review experimental progress on a few selected protein systems.

4. Photosynthetic proteins

4.1. Vibrational coherence in bacterial reaction centers

The function of the photosynthetic reaction center (RC) membrane protein of purple bacteria is to generate a transmembrane potential via electron transfer between a set of cofactors. Electron transfer is driven by the free energy of a singlet excited state, initially generated by optical excitation. Therefore, the most apparent response to a physiological trigger (absorption of a photon) lies in the changes of the *electronic* configuration of the system. Nevertheless, the bacterial reaction center constituted the first protein in which nuclear motions were directly observed, as oscillatory modulations of the femtosecond kinetics of the primary donor excited state P*, at cryogenic temperature [27]. These initial studies were performed on isolated functional RCs from *Rhodobacter sphaeroides* R26 and on membrane-bound RCs from the D_{LL} mutant of *Rhodobacter capsulatus*, which is devoid of the primary acceptor bacteriopheophytin H_L and therefore does not perform electron transfer. The latter system displayed a relatively simple (two main frequencies at 15 and 77 cm^{-1}) oscillatory pattern in the stimulated emission spectral region and a detailed study of the spectral characteristics allowed to exclude the possibility that other phenomena, in particular electronic coherence, were at the origin of those signals [22]. In wild-type membrane-bound RCs of *R. sphaeroides*, the distribution of the fundamental frequencies of the activated modes was found to be more complex [32], with at least seven modes in the experimentally accessible (pulse duration limited to $< \sim 350$ cm^{-1}) low-frequency region, the three strongest occurring in the 90–160 cm^{-1} region. The oscillatory features are very similar when measured

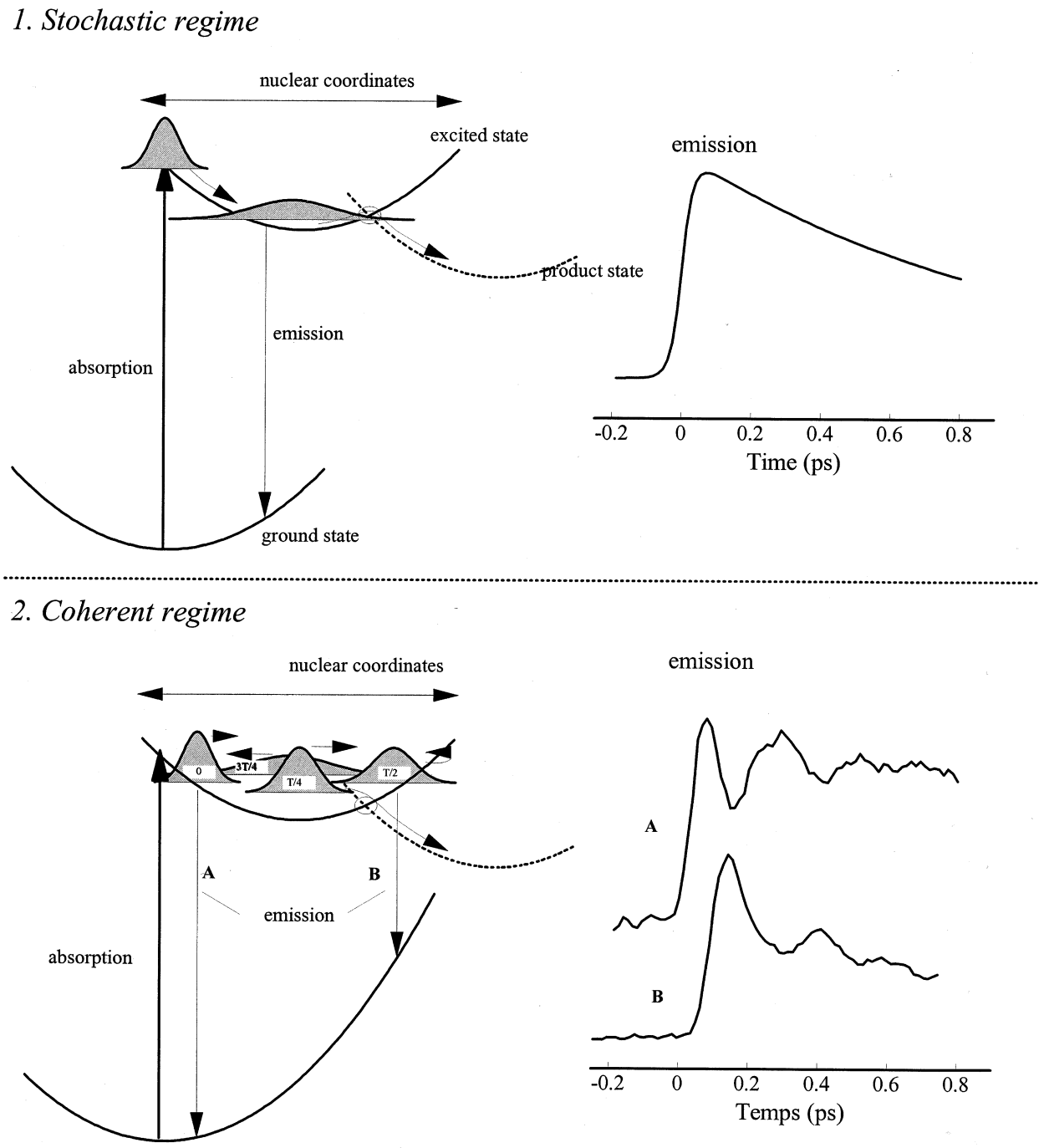

Fig. 2. Regimes of nuclear motions, illustrated by wave packet evolution on one-dimensional cross sections of excited state potential energy surfaces. (1) In the stochastic regime, the initially created wave packet rapidly relaxes towards a quasi-stationary distribution. The emission kinetics are monotonically decaying and wavelength-independent. Surface crossing towards a product state occurs by thermal population of the transition state. (2) In the coherent regime, the initially created wave packet moves back and forth. The emission kinetics are modulated with the frequencies of the motions and are wavelength-dependent, with opposite phases at both sides of the spectrum. Surface crossing can occur by thermal or by coherent motion along the reaction coordinate.

with stimulated emission (in a transient absorption configuration, see Section 2) [32] and with spontaneous emission [16], in agreement with their assignment to activated modes in the primary donor excited state (P*). At low temperature, the damping of the oscillatory features in WT RCs occurs concomitantly with the decay of the P* population in ~1 ps (see Section 4.4). Comparison with mutant RCs with longer-lived P*, shows that for most modes, the intrinsic dephasing time has a lower limit of ~2 ps [33]. The frequency spectrum corresponds well with the P-Raman-active modes [34,173,174] and the phonon distribution needed to fit hole-burning data [35], indicating that essentially all of the activated modes maintain phase relationships on the time scale of a few picoseconds. It was further demonstrated that this is also the case at room temperature [36]. The lower relative amplitude of the coherence signal at higher temperatures is primarily due to the fact that ground state motions are Boltzmann-activated, leading to an initially 'fuzzy' quantum excited state, characterized by a large spread in nuclear coordinates and phases in the initially populated wave packet [22,37].

The appearance of strongly activated directed coherent motions in an electron transfer-catalyzing protein is intriguing. It has been discussed by several groups [27,32,38–44] whether these coherent motions play a functional role (see also Section 4.4). Nuclear conformation changes may assist electronic reactions, but a spectroscopic assessment of a direct role of coherent motions in primary electron transfer is not straightforward [23] (see Section 4.4). Moreover, the detailed characteristics of these motions are essentially unknown. The following observations give more general indications for their nature.

4.2. *Characteristics of low-frequency vibrations in photosynthetic proteins*

The primary electron donor P is a bacteriochlorophyll dimer (Fig. 3) and the P* state has intradimer charge transfer (of the type $P_L^+P_M^-$) character [45], which could provide a way to Franck–Condon couple intradimer modes. This suggests that at least some of the vibrational modes involve relative motions of the two halves of the dimer. Pioneering work by Warshel using molecular dynamics simulations of model dimers suggests an intra-dimer vibrational frequency of ~100 cm^{-1} [46]. Vibrational coherence has not been observed in bacteriochlorophyll monomers [47]. Apart from reaction centers, low-frequency vibrational coherence has now also been observed in the excited states of a variety of antenna systems, mostly (but not exclusively [48]) bacteriochlorophyll-containing complexes. Observations of coherences in complexes from purple bacteria include the core light-harvesting antenna (LH-1) of both bacteriochlorophyll *b* [49] and bacteriochlorophyll *a* containing species [30,50,51] (main frequency ~105 cm^{-1}) and the B820 unit which is derived from it [52,53] (main frequency 170 cm^{-1}) as well as the peripheral light-harvesting antenna (LH-2) [30,54] (main frequency ~150 cm^{-1}, much weaker than LH-1). Coherences have also been reported in complex systems from green bacteria, including the chlorosome [55] (many frequencies near 50 and 100–250 cm^{-1}) and, interestingly (see below), the Fenna–Matthews–Olson (FMO) complex (main frequency 110 cm^{-1}) [56]. The appearance of low-frequency coherence in bacteriochlorophyll assemblies which are thought to have dimeric interactions, and the analogy to the assignment of the ~130 cm^{-1} vibrational progression observed in hole-burning of the primary donor dimer in bacterial RCs [57] to a dimer mode, has led to the suggestion that these motions correspond to intradimer vibrational modes [51,52]. This suggestion is generally consistent with the idea that formation of a delocalized electronic excited state activates these motions. Yet several arguments indicate that these modes should not be regarded as pure dimer modes.

(1) It is likely that, at least for the FMO complex (a '21-mer') and LH-2 (see Section 4.5), the excited state is delocalized over more than two bacteriochlorophylls. For LH-1, the coherences appear more pronounced and less frequency-dispersed, which may indicate more localization within a dimer unit [51], however in the B820 complex, which is thought to contain separated LH-1 dimers, the main frequency component has shifted from ~105 cm^{-1} to ~170 cm^{-1} [52,53] and the frequency spectrum is more dispersed. On the other hand, indications that low-frequency motions might be confined to a monomer come from the recent reports of low-frequency (down to ~60 cm^{-1}) resonance Raman

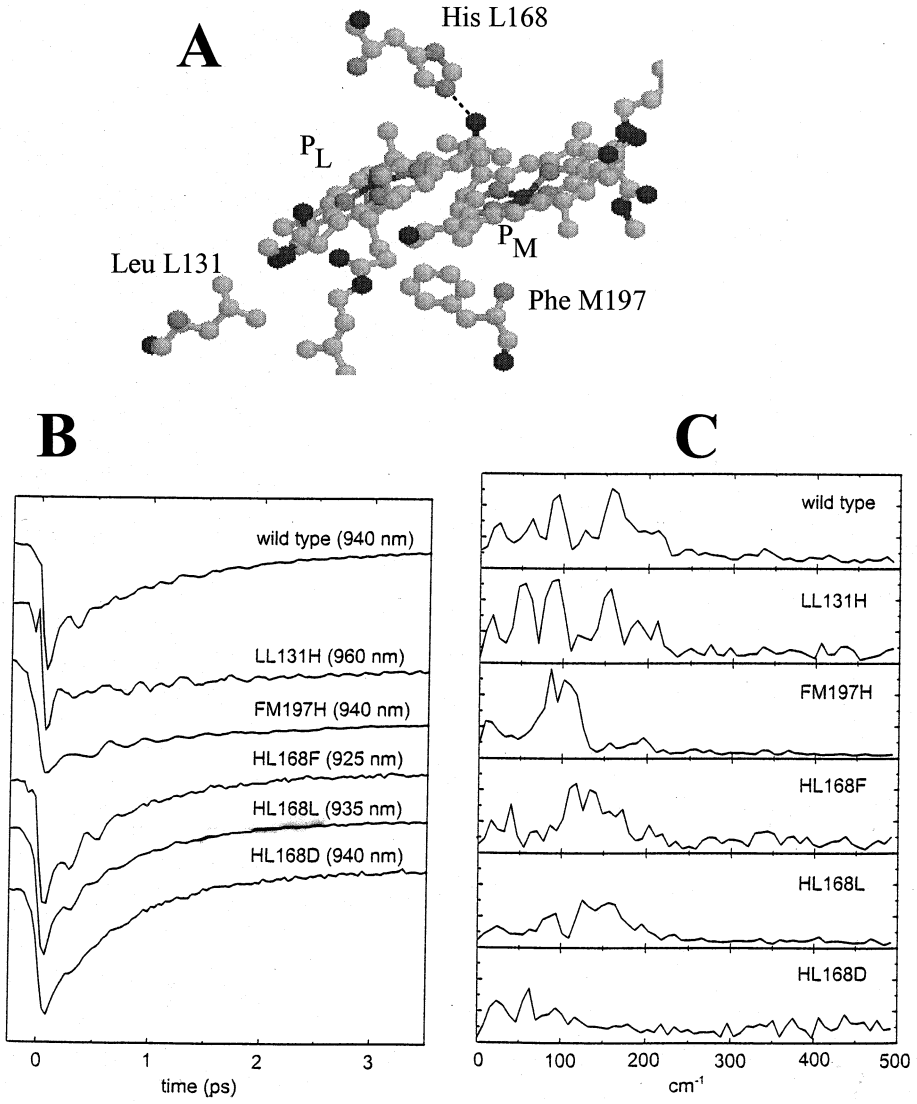

Fig. 3. Influence of hydrogen bonds between the bacteriochlorophyll dimer P and the protein in reaction centers of *Rhodobacter sphaeroides* on the vibrational motions coupled to the $P \rightarrow P^*$ transition [61]. (A) View of the bacteriochlorophylls P_L and P_M and three residues that were altered by site-directed mutagenesis. In wild-type RCs, a hydrogen bond is present between P_L and His L168 (dotted line). This hydrogen bond can be broken by introducing Phe, Leu or Asp at position L168. Additional hydrogen bonds can be added by introducing His at position M197 or L131 (or M160, not shown). (B) Stimulated emission kinetics at selected wavelengths recorded at the red side of the emission band at 18K in wild-type and various mutant RCs. (C) Fourier transforms of the oscillations in the kinetics of panel B, representing the fundamental frequency spectra of the vibrational modes set in motion by excitation of P. The drastic variations of the spectra indicate involvement of the protein in the chromophore vibrational modes. Panels B and C are reprinted (with permission) from [61], copyright (1998) National Academy of Sciences, USA.

bands of dry bacteriochlorophyll films [34,58]. However, these may reflect delocalized multimer modes, as under these condition aggregation is likely to occur [59].

(2) For bacterial RCs, the frequency spectrum is quite different for WT RCs of *R. sphaeroides* [32], (many frequencies, mainly in the 90–160 cm^{-1} region) and for the D_{LL} mutant of *R. capsulatus* [22] (two main frequencies at 15 and 77 cm^{-1}). Whereas the manifold of differences between the two types of RCs prohibits a detailed comparison, this indicates that the vibrational modes are not localized within the bacteriochlorophyll cofactors or within the dimer. Furthermore, slight differences in damping

of the vibrational modes, activated by optical excitations, have been observed between detergent-isolated and membrane-bound RCs [60]. This also indicates that the protein matrix is involved in these motions.

(3) In a more systematic study of RCs from *R. sphaeroides*, we have recently reported substantial changes in the frequency spectrum induced by single-site mutations altering the hydrogen bond pattern between P and the protein [61] (Fig. 3). A comparison with the charge distribution in the P^+ state of these mutants [62], together with the lack of frequency shifts upon changing of the electronic configuration of P by various mutations at position M210 [33], strongly suggest that perturbations of vibrational modes are involved, including the protein. The alterations were stronger for interactions in the vicinity of the overlap area of the two bacteriochlorophylls, indicating that dimer-type motions are likely contributing to the affected modes.

In conclusion, it appears that the low-frequency coherent motions in photosynthetic complexes, activated by the formation of the excited state (the electron donor state P* for RCs), can be identified as chromophore-driven protein motions.

4.3. Vibrational coherence and energy transfer

In electron-transfer catalyzing photosynthetic systems, in vivo photochemistry follows energy transfer from an antenna system. Dynamics of energy transfer has been reviewed by van Grondelle and coworkers [63] and, with the exception of one recent development (Section 4.5), will not be reviewed in detail here. Yet a few aspects are of considerable interest in the framework of the vibrational coherence discussed above.

First, coherent motions in RCs have been studied mainly upon direct excitation of the lowest-lying excited state P* of the system. A question is whether such motions are also activated when P* is formed by downhill energy transfer, from other electronic states in the RC, or from the surrounding antenna. It has recently been shown [64,65] that this is the case for energy transfer, in the 50–200 fs time scale, from the B* and H* excited states of the monomers of the RC cofactor system, indicating that the nuclear configuration along the P*-active modes is not much modified prior to P* formation. Antenna excited states will probably influence the RC configuration to an even lesser extent than B* and H*. Therefore, upon P* population via energy transfer from the antenna, the same motions are presumably activated as upon direct P* formation in antenna-devoid complexes (however, this cannot be directly investigated because the energy transfer times are too slow (tens of picoseconds) to effectively synchronize the motions). This indicates that these motions accompany electron transfer also under physiological circumstances.

Second, an intriguing observation is that in several antenna systems where energy transfer occurs between isoenergetic states, vibrational coherence is maintained on a time scale several times longer than the average 'hopping time' between such states [30,49,66]. This clearly indicates that a Förster-type description, assuming vibrationally relaxed states, is not valid for the energy-transfer process. The phenomenon that the coherences are transferred with the excitation suggests that either the transfer is modulated by the vibrational modes or that the interacting states are strongly delocalized and involve the same pigments. A full comprehension of such transfer processes must await developments of theoretical models including nonthermal nuclear dynamics.

We note that vibrational coherence has not been observed in strongly heterogeneous antenna systems like those of heliobacteria [67,68] and Photosystem I [69]. This does not a priori exclude coherent energy transfer, but the spectral inhomogeneity of such systems may wash out any coherent mechanisms.

4.4. Electron transfer in bacterial reaction centers

Ultrafast electron transfer has been studied in a variety of RC complexes. The bacterial RC in its isolated or antenna-depleted membrane-bound form constitutes a model system for biological electron transfer. The reactant state (P*) can be generated by direct and exclusive excitation of the primary donor P. After the early assessment of roughly concomitant decay of P* and appearance of the product state $P^+H_L^-$ in $\sim$3 ps at room temperature [17,70–72] and $\sim$1 ps at cryogenic temperature [73], much research has been focused on the role of the Bchl monomer B_L, which is located in between P and

H_L. The different approaches to this question have been extensively reviewed elsewhere [74–78]. Briefly, a direct reaction $P^* \rightarrow P^+H_L^-$ would be orders of magnitudes faster than predicted by classical nonadiabatic Marcus theory of electron transfer [79,80]. Therefore it has been proposed that the $P^+B_L^-$ serves as an intermediate, either as a real, transiently populated, intermediate or as a virtual intermediate via a superexchange mechanism [81,82]. In the former case, the decay of this state must be significantly faster than its formation to explain the similar kinetics of P* decay and $P^+H_L^-$ formation. Based on analysis of small transient features, an exponential scheme

$$P* \xrightarrow{k_1} P^+B_L^- \xrightarrow{k_2} P^+H_L^-$$

has been proposed by Zinth and coworkers [83,84], (somewhat more elaborate variations of this scheme have later also been proposed [85–87]), with k_2 1/0.9 ps at room temperature and 1/0.3 ps at cryogenic temperature [88] (however, low-temperature transients corresponding to the latter were not observed in our laboratory [89]). More generally this would imply that the $P^+B_L^- \rightarrow P^+H_L^-$ reaction takes place on a faster time scale than vibrational relaxation of the P* state [22,27,32,36], indicating that a reasoning in terms of thermally equilibrated states is a priori not valid. Therefore, it has also been proposed that the reaction occurs in a near-adiabatic regime, in which the potential energy surfaces of the states P*, $P^+B_L^-$ and $P^+H_L^-$ (and possibly other states, see below) are strongly coupled [27,32,38]. The temperature dependence of the P* decay reaction also points in this direction, as analysis in terms of a nonadiabatic single-mode model with a thermal distribution of vibrational levels, yielded a 'reaction' mode of ~ 80 cm^{-1} [73,88]. This would imply a near-adiabatic regime, at least at low temperature. Whether a single mode is coupled to the electron transfer reaction is an open question. The observation of coherent motion activated by P* formation (see above) suggests that the reaction coordinate is along one of these modes, yet the spectroscopic determination of such a mode is not straightforward [23,41]. For the dominant modes in the 90–160 cm^{-1} range, the spectroscopic features in the P* stimulated emission range do not suggest a strong direct coupling to primary electron transfer [23,90]. For the lower frequency range, the situation is less clear [23]. Involvement of 10 and 30 cm^{-1} modes in $P^+B_L^-$ formation has been suggested [41] on the basis of their appearance in a highly congested spectral region, but the mechanism of this involvement is unclear and furthermore the corresponding oscillations appear to persist beyond the proposed lifetime of this state.

In intact RC-antenna systems, the lowest-lying excited state P* is the precursor of electron transfer [63]. A novel set of observations concerns electron transfer in antenna-depleted systems, via other pathways as those outlined above. It has been thought that upon excitation of higher-lying states than P*; i.e., H*, B* or P_+* (P_+ denoting the higher exciton component of the dimer P), the excitation rapidly (on the time scale of 50–200 fs [64,65,70,91–93]) cascades down to the P* state, from which primary electron transfer proceeds. Yet, recently several groups have reported experiments on mutant [94,95] and wild-type [65,96–98] reaction centers indicating that part of the B* or H* excitations lead to charge separation through pathways bypassing P* formation. Spectral analyses indicate that radical pairs having a $P^+B_L^-$ or $B_L^+H_L^-$ character are formed en route towards the state $P^+H_L^-$ [65,95,98], although the formation of a substantial population of $B_L^+H_L^-$ is not observed in a mutant devoid of P [99], suggesting that the presence of P is a prerequisite for electron transfer in all cases. Whereas kinetic analyses are often performed in terms of exponential reactions between distinct states, it is possible that the electron transfer reaction(s) proceed by relaxation of the initially populated 'hot' excited states via a manifold of pathways on an adiabatic potential energy surface, coupling the surfaces of the involved excited and radical pair states, towards an electronic state with predominant $P^+H_L^-$ character [96].

Studies of electron transfer in other types of RCs are considerably complicated by the fact that P cannot be exclusively excited, leading to a spectroscopic evolution reflecting both electron transfer and energy transfer, which may take place on the same time scale. This is particularly the case for the Photosystem II RC, which is thought to be structurally similar to the bacterial RC, but where the absorption bands of all of the eight chlorins contained in the RC strongly overlap. It has been suggested that in this

case the primary donor is highly delocalized over an ensemble of pigments (see, for instance, [100]).

4.5. Energy transfer in LH2

An important novel stimulus for the study of structure/function relationships in antenna systems has come from the assessment that the antenna systems in purple bacteria are organized in ring-structures [2,101,102]. In particular, in the LH2 structure of *Rps. acidophila*, reported in 1995 [2], the 'B850' (absorbing near 850 nm) complex is organized in a ninefold symmetric ring of 18 strongly interacting Bchl *a* molecules, each pair of which is associated with a monomeric 'B800' (absorbing near 800 nm) Bchl *a* molecule. It had been known for several years that the downhill B800 → B850 energy transfer takes approximately 700 fs [103].

Much present research focuses on the role and functioning of the 'storage ring' arrangement of the B850 complex. A homogeneous 18-mer ring would give rise to delocalized degenerate excitations over the complex. Symmetry-breaking disorder can lead to more localized excitations. The main questions concern excitation energy transfer between the near-degenerate excited states of the complex and in particular the degree of delocalization ('coherence length', here coherence refers to *electronic* coherence) of the excitations over the various pigments. Using direct excitation into the B850 pool, the question has been studied with polarized absorption [104–107], polarized fluorescence [14] and 3-pulse photon echo spectroscopy [66] as well as with nonlinear absorption [108] and superradiance [109]. The data are analyzed in terms of models which include disorder and a description of high-lying electronic levels to account for excited state absorption. Values for the delocalization of the excitations ranging from 2–4 [14,66,105,107,109] to ∼18 pigments (the entire ring) [104,106,108,110] have been proposed. Part of these discrepancies might be traced back to the models used and to the definition and time scale of 'coherence length' probed by the various techniques. Also, different instrumental limitations may play a role; for instance Nagarajan et al. [104,111] report a very high (significantly above 0.4) initial absorption anisotropy decaying in 20–30 fs with ∼35 fs instrument response, whereas much lower values, both for the initial anisotropy (∼0.3) and decay rate (50–100 fs) were reported by Pullerits et al. [105] and Jimenez et al. [66] (in fluorescence) with an instrument response of ∼150 fs (note that interpretation of fluorescence is in principle more straightforward). Clearly, at present no consensus is reached on the determination of the coherence length and on the functional relevance of a ring-like structure and a unified interpretation framework is needed.

5. Retinal proteins

Two membrane-bound pigment–protein systems constitute the most well-known examples of systems in which an ultrafast light-induced conformational change takes place. These are rhodopsin, the photosensitive protein in vision [112], and bacteriorhodopsin, a protein which uses light to generate a proton gradient which drives photosynthesis in *Halobacteria* [113]. In both cases the primary process is the isomerization of a retinal chromophore bound to the protein, *trans* → *cis* for bacteriorhodopsin and *cis* → *trans* for rhodopsin.

5.1. Isomerization mechanism in bacteriorhodopsin

Bacteriorhodopsin is a photosynthetic retinal protein which functions as a light-driven proton pump in halobacteria [113]. Following the absorption of a photon by *all-trans* retinal, the initial event is its isomerization to the 13-*cis* form with a quantum yield of ∼65%. About a decade ago, several groups have shown that the ground state photoisomerized product appears in ∼500 fs [114–116], followed by the formation of a second intermediate in ∼3 ps.

The presently debated questions concern the shape and number of potential energy surfaces involved in the primary reaction (Fig. 4). Initially, in the blue part of the emission spectrum (< 750 nm), only very quickly decaying (100–200 fs) stimulated emission was observed [115,116] and this was interpreted as a rapid depopulation of the Franck–Condon region by motion along a strongly repulsive excited state potential energy surface [117]. In this view, isomerization takes place on the initially populated excited state. The 13-*cis* product ground state and the *all-trans* ground state are populated (and 'repopu-

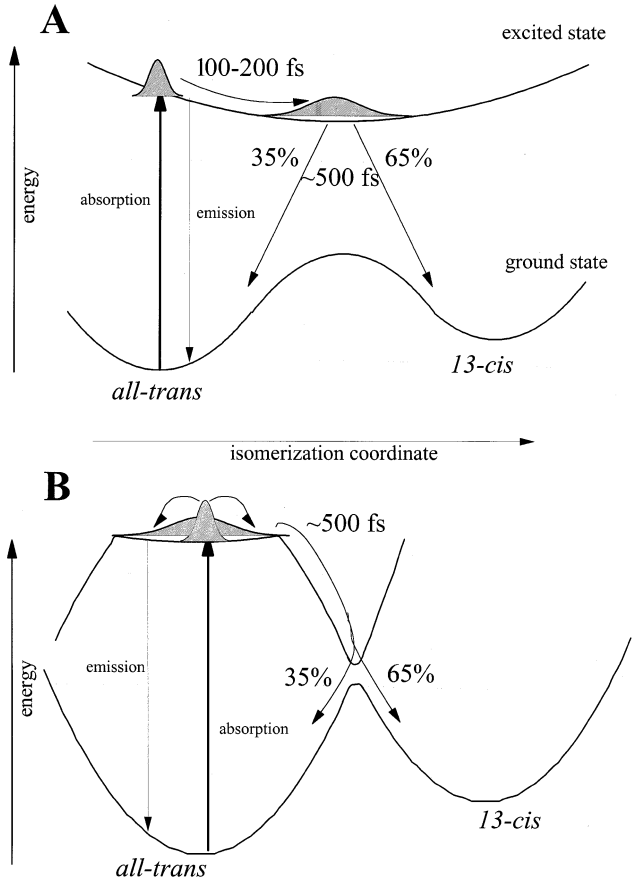

Fig. 4. Possible schemes for retinal isomerization in bacteriorhodopsin, roughly according to the ones proposed in [115] (A) and [119] (B).

lated' respectively) directly from the relaxed, excited state in ~500 fs, as monitored by decay of the stimulated emission on the red side of the emission band (> ~750 nm) [116].

However, several recent observations are at variance with the above picture. The time-resolved spontaneous emission was observed to occur with similar multiexponential kinetics throughout the very broad emission band, from 680 to 900 nm [118]. Two groups [119–121] have studied in detail the stimulated emission, including at the most red part of the emission band (>800 nm), and demonstrated that the blue part of the band is obscured by a compensating induced absorption, which explains the failure to observe broad-band stimulated emission in the early work [115,116]. In the more recent work [119–121] no spectral evolution of the spontaneous or stimulated emission was observed. Anfinrud and coworkers [119,120] (a similar mechanism was suggested by Hochstrasser and coworkers [121]) interpreted their results in terms of a three-state model inspired by molecular dynamics simulations [122], in which ultrafast equilibration (< 30 fs) takes place on the relatively flat excited state potential energy surface along the reaction coordinate. From this surface, crossing was proposed to occur, in ~500 fs, towards a strongly repulsive potential energy surface, from which the product and reactant ground states are populated very rapidly. In this view, isomerization is driven by protein motions which are not directly coupled to the initial excitation of the retinal. This model could be better reconciled with a slight activation energy deduced from the decreasing rate of the isomerization reaction at low temperature (with a similar quantum yield) reported ~20 years ago with picosecond pulses [123]. Yet more recent results using pulses of 350 fs indicate that the reaction is essentially temperature independent down to 20K [124], consistent with an activationless mechanism. Another difficulty with the three-state model (Fig. 4B) is that it does not explain the 100–200 fs spectral evolution observed previously near the Franck–Condon region [115,116]. Haran et al. [121] suggested this phase to be related to a change in energy between the initially created excited state and the higher-lying states.

Studies with bacteriorhodopsin mutants have been performed with the aim to unravel the mechanism of this reaction in more detail and on a molecular level. Specifically, a slower reaction with a similar quantum yield has been reported for several single-site mutants affecting the charge distribution in the vicinity of the chromophore [125–127], indicating that the shape of the isomerization potential energy surface depends on the environment. To test the validity of the different possible models, it is warranted to extend these studies to lower temperatures, as discussed by Logunov et al. [127], and to higher time resolution.

5.2. Vibrational coherence in bacteriorhodopsin

Using short probe pulses (12 fs), high-frequency (> 1000 cm^{-1}) vibrational coherences have been observed in bacteriorhodopsin, in the spectral region where the ground state absorbs [28]. These have been interpreted as motions on the ground state po-

tential energy surface activated by the impulsive stimulated Raman effect [24,28]. The spectrum corresponds to that expected from the ground state resonance Raman spectrum, indicating that all activated motions are underdamped. This work constituted the first evidence for ISR in a protein system (later it was reported for heme proteins [29] and bacterial RCs [30]). Such a coherent spectroscopy constitutes an interesting tool to characterize ground-state motions, yet without enlightening us on their possible functional role.

In contrast to rhodopsin (see Section 5.3), in bacteriorhodopsin no coherence has been reported in relation to formation of the isomerized product state. This may be related to the relatively slow speed of isomerization.

5.3. Rhodopsin

The cascade of events constituting the vision process is initiated in rhodopsin. A photon is absorbed by the 11-*cis* retinal chromophore, which subsequently isomerizes to the all-*trans* configuration (bathorhodopsin) via dissipation of approximately 40% of the photon energy [112]. This process has a quantum yield of 67% [112,128], the remainder returns to the 11-*cis* ground state. The reaction has a well-defined reaction coordinate, the torsion along the (11,12) bond. Early picosecond spectroscopic studies have been reviewed by Schichida [128]. Here we will focus on femtosecond work, which has been produced only since 1991 on rhodopsin [129,130].

Much work has been done by Mathies, Shank and coworkers [130–132], using visible transient absorption spectroscopy. The overall kinetics show main phases of $\sim$200 fs and a few ps, superimposed on which appear strong oscillatory features, indicating that the reaction occurs in a regime of vibrational coherence (see below). Following bleaching of the ground state band centered at $\sim$500 nm, in $\sim$200 fs an induced absorption appears at wavelengths $>$560 nm, presumably reflecting the isomerized retinal. This observation has been interpreted [130,131] as the consequence of the formation of the bathorhodopsin product state directly in its ground state via an adiabatic surface crossing, using a similar model to that proposed for bacteriorhodopsin (see Section 5.1). In the same framework, the further spectral relaxation, including a blue shift of the induced absorption band towards the known maximum of this state at $\sim$550 nm, reflect further conformational relaxation and vibrational cooling, both in the rhodopsin reactant and bathorhodopsin product ground states.

Based on early single wavelength kinetics with a lower time resolution in which coherences were not observed, an alternative interpretation was given by Callender and coworkers [129]. They suggested that the 200-fs phase reflects isomerization on the excited state potential energy surface followed by relaxation to the bathorhodopsin ground state in $\sim$3 ps. However, the later full spectral data of Peteanu et al. [131] and Wang et al. [132] strongly suggest that the bathorhodopsin product state is formed directly in $\sim$200 fs.

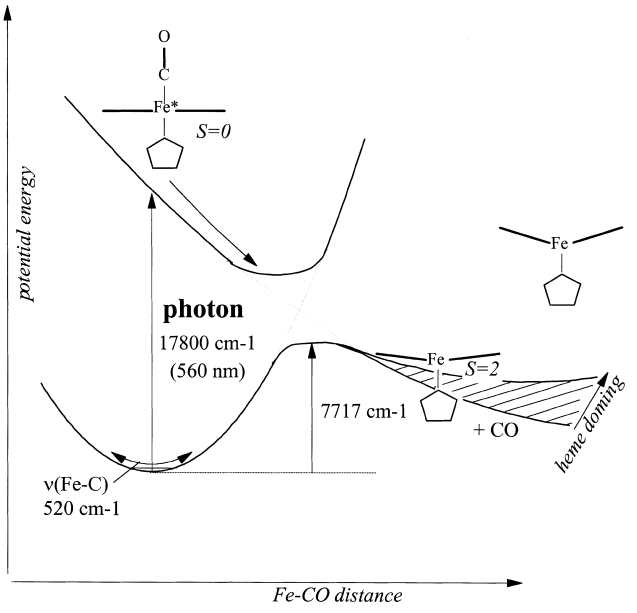

Fig. 5. Scheme of potential energy surface cross sections along the reaction coordinate of ligand (here CO) dissociation in heme proteins. Absorption of a photon by the liganded, low-spin heme leads to motion along a repulsive excited state surface. The dissociation energy is approximately 22 kcal/mol (7717 cm^{-1}) [172], which is lower than the heme's lowest electronic transition with sizable oscillator strength. Along with photodissociation, the Fe spin changes and heme doming towards the distal histidine occurs, by motion in a direction perpendicular to the dissociation coordinate [148]. Heme doming ($\nu\sim$50 cm^{-1}) presumably occurs an order of magnitude slower than dissociation ($\nu\sim$520 cm^{-1}).

In rhodopsin, strong oscillations are observed in the transient absorption experiments [130,132]. The spectroscopic properties of features with a main frequency of $\sim$60 cm^{-1} (period 550 fs) were studied in detail by Wang et al. [132]. They demonstrated that these reflect coherent vibrational motion on the potential energy surface of the product, bathorhodopsin, state. Apparently, the product state formation is fast enough ($\sim$200 fs) for coherent population of the 60 cm^{-1} mode; in accordance, no coherent motions are clearly observed in isorhodopsin, where a slower isomerization (along the 9–10 torsional coordinate) in $\sim$600 fs occurs [133]. The visualization of a product state mode of which the quarter period (130 fs) corresponding approximately to the reaction time, suggests that the mode is strongly coupled to the reaction [132]. Unfortunately this suggestion is difficult to prove, as due to its very short lifetime (a fraction of the period of the putative coupled mode) coherence in the reactant state cannot be studied. The close correlation between isomerization speed and quantum yield in rhodopsin and two analogs [133,134] led Mathies, Shank and coworkers to support a ballistic curve-crossing mechanism for the reaction (although wave packet broadening apparently also plays a role in the case of 13-demethyl rhodopsin [134]). This suggests that the frequency of the 'reaction mode' is also different in these species, which may provide a means to further characterize the 'molecular identity' of this mode.

6. Heme proteins

Heme proteins play an essential role in a wide variety of physiological functions, by their capacity to bind and release external ligands or by their redox properties, or both. Photoactivation of heme proteins is not a natural process, however small ligand like CO, O_2, or NO (but not CN), bound to the heme iron, can be photodissociated in the femtosecond time scale with a very high quantum yield [1,135,136], and this provides a unique property to synchronize the dissociation of ligands and subsequently study the dynamics of the system. The early photophysical processes involve two excited states, decaying on a time scale of a few hundred femtoseconds and a few picoseconds, respectively. These states have been spectroscopically characterized for myoglobin and hemoglobin [135,137]. They have been reviewed previously [1] and appear to follow a similar scheme in a variety of proteins, including cytochrome *c* oxidases aa_3 [138] and cbb_3, quinol oxidase *bd*, NO synthase, and cytochrome *b* and *c* (unpublished results), with some variation in the lifetimes and relative populations of the two excited states.

The dynamics of geminate recombination of external ligands after photodissociation have been studied on the picosecond time scale as an indirect probe of the protein rearrangements on this time scale. This has been done in particular with NO as a ligand, in which case a major fraction of the heme-ligand pairs recombine within a few hundred picoseconds. Strongly nonexponential recombination is observed [139,140], likely at least in part reflecting a relaxation of the protein on the time scale of recombination. Using site-directed mutants of myoglobin [141,142] residues have been identified that affect the recombination process on the picosecond time scale, some of which are surprisingly remote from the heme [141].

6.1. Vibrational dynamics

Recent research has focused on the direct evaluation of the heme and protein conformational dynamics following ligand detachment. The dissociation of the ligand presumably occurs within half a period of the Fe–ligand stretching frequency ($\sim$520 cm^{-1} for Fe–CO); i.e., in less than 50 fs [1] (Fig. 5). An important question is how and on what time scale the heme and the protein accommodate to this change. Spectroscopically, information on the heme reaction is most straightforward to obtain. For hemes with a 6-coordinate heme iron, photodissociation of one ligand results in a 5-coordinate heme iron and relative motion of the iron out of the heme plane ('doming'). The vibrational frequency of the heme-doming motion in myoglobin has been suggested to be $\sim$50 cm^{-1} [26,143,144]. Hence the lower limit of the speed of heme doming is $\sim$170 fs (a quarter of a period). Time-resolved resonance Raman studies of the Fe–His mode ($\sim$220 cm^{-1}) have demonstrated that upon photodissociation of CO–hemoglobin and CO–myoglobin, heme doming occurs essentially in less than 1 ps [12,145]. More recent very high signal

to noise transient Raman data in the high-frequency regions are in agreement with this view [13]. Measurements of the shift of the position of the band III charge-transfer absorption band in myoglobin have been interpreted to reveal a substantial additional ($\sim$20%) doming on the time scale of tens and hundreds of picoseconds [146,147]; yet as discussed by Franzen et al. [145], protein relaxations may influence the position of this band as well.

Recently, femtosecond coherence spectroscopy has been used to study the coherent reaction of the heme upon impulsive excitation of cytochrome *c* and myoglobin. Champion and coworkers [29,148] pioneered such an approach using both excitation and probing in the Soret band. As the Soret band is strongly Raman active for the low-frequency modes [149], these excitation conditions lead to strong impulsive stimulated Raman signals (wave packet motion on the *ground* state) and indeed the observed frequencies correlated well with the Raman spectrum [29]. Furthermore, for the case of MbNO, where the excitation pulse in addition leads to dissociation of the NO ligand, low-frequency motions assigned to Fe–His stretching (220 cm^{-1}) and heme doming (75 cm^{-1}, but see [26]) have been observed in single wavelength kinetics and assigned to the deliganded product state [148]. This result was interpreted in terms of the very rapid photodissociation which sets in motion these modes (cf. Fig. 5), suggesting the importance of these modes in the heme-ligand interaction. This technique thus appears powerful both as a tool for vibrational spectroscopy in the low-frequency domain and to investigate the functional importance of motions coupled to the reaction. The study of the latter aspect may be considerably facilitated by the use of excitation conditions which are not Raman active for the investigated modes. This should avoid complications arising from the superposition of the two types of signals. With this aim, multicolor spectroscopic experiments using impulsive excitation in the heme α band are currently carried out in our laboratory.

The trajectory of the dissociated CO–ligand from MbCO has also been investigated by polarized transient infrared spectroscopy [150]. Evidence was presented for the transfer to two spectroscopically distinct antiparallel docking positions, parallel to the heme plane, with different time scales of 0.2 ps and 0.5 ps. A comparison with classical diffusion dynamics indicated that the motion leading to these positions is inertial; i.e., directed. We note that the time scale of these processes is similar to that proposed for the major rearrangement of the heme, heme doming ($\sim$50 cm^{-1}, see above, corresponding to a period of $\sim$0.7 ps). This suggests that, upon breaking of the heme–ligand bond, the motion of the heme, and the trajectory of the ligand (thought to be predominantly along the heme plane [150]) remain correlated and possibly concerted. In the same study [150], a strong, near threefold, increase in the absorption of the CO-stretch occurring in $\sim$1.6 ps, was assigned to reflect the protein response to the occupancy of the docking site. In this view, local protein accommodation occurs as a delayed response to the arrival of CO in the site, but occurs prior to heme and CO vibrational relaxation (see Section 6.2).

6.2. Vibrational relaxation

Generally, the assessment that vibrational coherence for the low-frequency modes is maintained for a few picoseconds in proteins, even at room temperature, demonstrates that the biochemistry on this time scale takes place in a mixed regime of coherent and stochastic motions. The dephasing times of the oscillatory features set a *lower limit* for vibrational dephasing and relaxation of $\sim$2 ps (intrinsic inhomogeneity may also lead to dephasing). Accordingly, the time required for vibrational energy dissipation upon optical excitation of the heme has been estimated in the picosecond time range by various methods. Mituzani and Kitegawa [13], using picosecond anti-Stokes resonance Raman spectroscopy, have recently determined the cooling of the heme by dissipation of the excess energy stored in the ν_4 mode ($\sim$1350 cm^{-1} in deoxymyoglobin, arising from in-plane heme vibrations) upon photodissociation of MbCO. They found biphasic cooling with temperature-decay times of 3 ps (93%) and 25 ps (7%), in agreement with earlier anti-Stokes work with a lower time resolution [151] and with an earlier detailed analysis of the time evolution of the Stokes-band [11]. This finding is in general agreement with the limits observed by coherence spectroscopy, although it should be kept in mind that the energy dissipation for low-frequency modes may be slower than for

high-frequency modes. From transient infrared studies, the heating of the D_2O solvent upon exciting the hemes in (unliganded) hemoglobin and myoglobin was found to be substantially slower (main phase of $\sim$8 ps) [152], suggesting that the flow of energy from heme to the aqueous solvent passes via the protein moiety.

Vibrational relaxation and vibrational dephasing upon direct excitation of CO in the CO-stretching mode (around 1950 cm^{-1}, depending on the protein) in MbCO has also been measured using infrared pump-probe [153,154] and vibrational echo [15,155,156] spectroscopy. Vibrational relaxation takes $\sim$20 ps, depending somewhat on the orientation of CO with respect to the heme [153,154] and presumably proceeds via the CO-heme bond. Comparison with the above-discussed dynamics of heme cooling and the result that the binding of the heme to the protein via the covalent Fe–proximal histidine bond does not affect vibrational dephasing [156], indicate that energy dissipation via the CO–Fe bond is rate limiting in this case.

6.3. Oxidases

Many of the studies on heme proteins have been performed on the 'model proteins' myoglobin and, to a less extent, hemoglobin. These studies can serve as an interpretation framework for the ultrafast chemistry in many other hemeproteins with a large variety of biological functions. In particular, studies have been performed on cytochrome *c* oxidase aa_3, a key enzyme in the respiratory chain which catalyzes the 4-electron reduction of molecular oxygen to water. The crystal structures of this membrane protein from bovine heart [4] and its bacterial counterpart [5] have recently become available. The oxygen binding site, heme a_3, is located in close proximity ($\sim$4.5 Å) to one of the two copper centers, CuB and a cross-linked histidine–tyrosine structure [157]. This particular arrangement is probably of great importance for the catalytic function of the enzyme. Ultrafast studies, previously reviewed by Einarsdottir [158], have thus far only been carried out with CO as a ligand, as O_2-liganded complexes cannot be generated in steady state. Upon excitation of the hemes, CO dissociates from heme a_3 within 100 fs [138], and subsequently binds to CuB in less than 1 ps [159,160], from where it leaves the complex on a microsecond time scale. The transfer of CO to CuB thus provides an example of a highly directed short-range transfer of a ligand. Femtosecond coherence spectroscopic measurements will be very useful to investigate the vibrational modes involved in this reaction. Whether CuB also is involved directly in transient binding of O_2 in the functional enzyme is unclear, yet a peroxide ligand has been suggested to bridge the a_3-CuB space in the 'as-prepared' enzyme [157].

The proximal coordination of the heme a_3 upon photodissociation of CO has been subject to considerable debate. Woodruff [161] proposed a mechanism in which the transfer of CO to CuB induces a ligand residue which coordinates CuB to switch and replace the proximal histidine bonded to heme a_3 in $\sim$6 ps (corresponding to a relaxation phase observed in transient absorption measurements [138]). This ligand-shuttle mechanism was proposed to play a role in controlling the access of external ligands to the active site and the rate of through-bond electron transfer towards the active site, as well as in proton pumping. However, the later available crystal structures show no obvious candidates for such a 'switch' ligand-residue. Recent picosecond resonance Raman experiments [162] have demonstrated that the Fe–His mode ($\sim$220 cm^{-1}) is observed within 5 ps after CO dissociation, implying that a histidine ligand is present at this time scale. Although in principle it cannot be excluded that the present proximal histidine is replaced by another histidine (CuB is coordinated by three histidines) in less than 5 ps, the authors strongly favor a mechanism in which the proximal coordination of heme a_3 remains unchanged. Future transient Raman experiments with a higher time resolution may further help to resolve this issue.

7. Concluding remarks

We have reviewed some of the recent developments in ultrafast studies, mainly focusing on primary processes in some more extensively characterized proteins. Yet ultrafast spectroscopy has become a tool for investigation of specific primary processes in a wide variety of photoactive proteins, including

for instance green fluorescent protein [163–165] and the plant growth regulation protein phytochrome [166,167]. Along another axis, modern ultrafast optical techniques are used to study more general aspects of protein physical chemistry. For example, three-pulse photon echo spectroscopy has been used to study spectral diffusion of heme groups as a probe for the energy landscape of proteins [168–170] and two-dimensional femtosecond infrared spectroscopy has been used to study vibrational energy flow in peptides [171].

A main general notion that emerges from the work of the last few years is that on the time scale of femtoseconds, the conformational changes that constitute or assist the function of a protein are highly directed and concerted motions. Many of these motions appear to take place on the time scale of 100 fs–1 ps. Present spectroscopic techniques monitor the projection of such motions on the spectroscopic observable. One ultimate goal will be to 'film' the protein structures in real time in the course of these motions. Technical progress towards this end has recently been made, resulting in the detection of femtosecond X-ray diffraction [21].

Acknowledgements

We acknowledge Jean-Christophe Lambry for help in preparing Fig. 3 and V. Nagarajan for providing a preprint of unpublished work. M.H.V. is supported by CNRS.

References

[1] J.-L. Martin, M.H. Vos, Annu. Rev. Biophys. Biomol. Struct. 21 (1992) 199–222.
[2] G. McDermott, S.M. Prince, A.A. Freer, A.M. Hawthornthwaite-Lawless, M.Z. Papiz, R.J. Cogdell, N.W. Isaacs, Nature 374 (1995) 517–521.
[3] W.-D. Schubert, O. Klukas, N. Krauss, W. Saenger, P. Fromme, H.T. Witt, J. Mol. Biol. 272 (1997) 741–769.
[4] T. Tsukihara, H. Aoyama, E. Yamashita, T. Tomizaki, H. Yamaguchi, K. Shinzawa-Itoh, R. Nakashima, R. Yaono, S. Yoshikawa, Science 269 (1995) 1069–1074.
[5] S. Iwata, C. Ostermeier, B. Ludwig, H. Michel, Nature 376 (1995) 660–669.
[6] F. Yang, L.G. Moss, G.N. Phillips, Nat. Biotechnol. 14 (1996) 1246–1251.
[7] K. Brejc, T.K. Sixma, P.A. Kitts, S.R. Kain, R.Y. Tsien, M. Ormö, S.J. Remington, Proc. Natl. Acad. Sci. USA 94 (1997) 2306–2311.
[8] H.-W. Park, S.-T. Kim, A. Sancar, J. Deisenhofer, Science 268 (1995) 1866–1872.
[9] B.R. Crane, A.S. Arvai, R. Gachhui, C. Wu, D.K. Ghosh, E.D. Getzoff, D.J. Stuehr, J.A. Tainer, Science 278 (1997) 425–431.
[10] A. Baltuska, Z. Wei, M.S. Pshenichnikov, D.A. Wiersma, Opt. Lett. 22 (1997) 102–104.
[11] J.W. Petrich, J.-L. Martin, D. Houde, C. Poyart, A. Orszag, Biochemistry 26 (1987) 7914–7923.
[12] S. Franzen, J.-C. Lambry, B. Bohn, C. Poyart, J.-L. Martin, Nature Struct. Biol. 1 (1994) 230–233.
[13] Y. Mizutani, T. Kitagawa, Science 278 (1997) 443–446.
[14] R. Jimenez, S.N. Dikshit, S.E. Bradforth, G.R. Fleming, J. Phys. Chem. 100 (1996) 6825–6834.
[15] C.W. Rella, K.D. Rector, A. Kwok, J.R. Hill, H.A. Schwettman, D.D. Dlott, M.D. Fayer, J. Phys. Chem. 100 (1996) 15620–15629.
[16] R.J. Stanley, S.G. Boxer, J. Phys. Chem. 99 (1995) 859–863.
[17] J.-L. Martin, J. Breton, A.J. Hoff, A. Migus, A. Antonetti, Proc. Natl. Acad. Sci. USA 83 (1986) 957–961.
[18] A. Bonvalet, M. Joffre, J.-L. Martin, A. Migus, Appl. Phys. Lett. 67 (1995) 2907–2909.
[19] M. Joffre, A. Bonvalet, A. Migus, J.-L. Martin, Opt. Lett. 21 (1996) 964–966.
[20] R.W. Schoenlein, W.P. Leemans, A.H. Chin, P. Volfbeyn, T.E. Glover, P. Balling, M. Zoloterev, K.-J. Kim, S. Chattopadhyah, C.V. Shank, Science 274 (1996) 236–238.
[21] C. Rischel, A. Rousse, I. Uschmann, P.-A. Albouy, J.-P. Geindre, P. Audebert, J.-C. Gauthier, E. Förster, J.-L. Martin, A. Antonetti, Nature 390 (1997) 490–492.
[22] M.H. Vos, F. Rappaport, J.-C. Lambry, J. Breton, J.-L. Martin, Nature 363 (1993) 320–325.
[23] M.H. Vos, M.R. Jones, J.-L. Martin, Chem. Phys. 233 (1998) 179–190.
[24] W.T. Pollard, S.L. Dexheimer, Q. Wang, L.A. Peteanu, C.V. Shank, R.A. Mathies, J. Phys. Chem. 96 (1992) 6147–6158.
[25] D.M. Jonas, S.E. Bradforth, S.A. Passino, G.R. Fleming, J. Phys. Chem. 99 (1995) 2594–2608.
[26] P.M. Champion, F. Rosca, W. Wang, A. Kumar, J. Christian, A. Demidov, in: P.M. Heyns (Ed.), Proceedings of XVIth International Conference on Raman Spectroscopy, Wiley, Chichester, 1998, pp. 73–76.
[27] M.H. Vos, J.-C. Lambry, S.J. Robles, D.C. Youvan, J. Breton, J.-L. Martin, Proc. Natl. Acad. Sci. USA 88 (1991) 8885–8889.
[28] S.L. Dexheimer, Q. Wang, L.A. Peteanu, W.T. Pollard, R.A. Mathies, C.V. Shank, Chem. Phys. Lett. 188 (1992) 61–66.
[29] L. Zhu, P. Li, M. Huang, T. Sage, P.M. Champion, Phys. Rev. Lett. 72 (1994) 301–304.
[30] M. Chachisvilis, T. Pullerits, M.R. Jones, C.N. Hunter, V. Sundström, Chem. Phys. Lett. 224 (1994) 345–354.
[31] L.D. Book, D.C. Arnett, H. Hu, N.F. Scherer, J. Phys. Chem. A 102 (1998) 4350–4359.

[32] M.H. Vos, M.R. Jones, C.N. Hunter, J. Breton, J.-C. Lambry, J.-L. Martin, Biochemistry 33 (1994) 6750–6757.
[33] M.H. Vos, M.R. Jones, J. Breton, J.-C. Lambry, J.-L. Martin, Biochemistry 35 (1996) 2687–2692.
[34] M. Lutz, Biospectroscopy 1 (1995) 313–327.
[35] P.A. Lyle, S.V. Kolaczkowski, G.R. Small, J. Phys. Chem. 97 (1993) 6924–6933.
[36] M.H. Vos, M.R. Jones, C.N. Hunter, J. Breton, J.-L. Martin, Proc. Natl. Acad. Sci. USA 91 (1994) 12701–12705.
[37] J.-L. Martin, J. Breton, M.H. Vos, in: D.A. Wiersma (Ed.), Femtosecond Reaction Dynamics, North Holland, Amsterdam, 1994, pp. 237–244.
[38] N.W. Woodbury, J.M. Pelloquin, R.G. Alden, X. Lin, S. Lin, A.K.W. Taguchi, J.C. Williams, J.P. Allen, Biochemistry 33 (1994) 8101–8112.
[39] A.M. Streltsov, A.G. Yakovlev, A.Y. Shkuropatov, V.A. Shuvalov, FEBS Lett. 383 (1996) 129–132.
[40] A.M. Streltsov, T.J. Aartsma, A.J. Hoff, V.A. Shuvalov, Chem. Phys. Lett. 266 (1997) 347–352.
[41] A.M. Streltsov, S.I.E. Vulto, A.Ya. Shkuropatov, A.J. Hoff, T.J. Aartsma, V.A. Shuvalov, J. Phys. Chem. B 102 (1998) 7293–7298.
[42] S.S. Skourtis, A.J.R. da Silva, W. Bialek, J.N. Onuchic, J. Phys. Chem. 96 (1992) 8034–8041.
[43] J.N. Gehlen, M. Marchi, D. Chandler, Science 263 (1994) 499–502.
[44] W.W. Parson, Z.T. Chu, A. Warshel, Photosynth. Res. 98 (1998) 147–152.
[45] E.J.P. Lathrop, R.A. Friesner, J. Phys. Chem. 98 (1994) 3056–3066.
[46] A. Warshel, Proc. Natl. Acad. Sci. USA 77 (1980) 3105–3109.
[47] S. Savikhin, W.E. Struve, Biophys. J. 67 (1994) 2002–2007.
[48] B.J. Homoelle, M.D. Edington, W.M. Diffey, W.F. Beck, J. Phys. Chem. B 102 (1998) 3044–3052.
[49] R. Monshouwer, M. Abrahamsson, F. van Mourik, R. van Grondelle, J. Phys. Chem. B 101 (1997) 7241–7248.
[50] M. Chachisvilis, V. Sundström, Chem. Phys. Lett. 261 (1996) 165–174.
[51] S.E. Bradforth, R. Jimenez, F. van Mourik, R. van Grondelle, G.R. Fleming, J. Phys. Chem. 99 (1995) 16179–16191.
[52] R. Kumble, S. Palese, R.W. Visschers, P.L. Dutton, R.M. Hochstrasser, Chem. Phys. Lett. 261 (1996) 396–404.
[53] W.M. Diffey, B.J. Homoelle, M.D. Edington, W.F. Beck, J. Phys. Chem. B 102 (1998) 2776–2786.
[54] T. Joo, Y. Jia, J.-Y. Yu, D.M. Jonas, G.R. Fleming, J. Phys. Chem. 100 (1996) 2399–2409.
[55] S. Savikhin, Y. Zhu, S. Lin, R.E. Blankenship, W.E. Struve, J. Phys. Chem. 98 (1994) 10322–10334.
[56] S. Savikhin, W.E. Struve, Photosynth. Res. 48 (1996) 271–276.
[57] S.G. Johnson, D. Tang, R. Jankowiak, J.M. Hayes, G.R. Small, J. Phys. Chem. 94 (1990) 5849–5855.
[58] J.R. Diers, D.F. Bocian, J. Am. Chem. Soc. 117 (1995) 6629–6630.
[59] J.R. Diers, Y. Zhu, R.E. Blankenship, D.F. Bocian, J. Phys. Chem. 100 (1996) 8573–8579.
[60] M.H. Vos, M.R. Jones, P. McGlynn, C.N. Hunter, J. Breton, J.-L. Martin, Biochim. Biophys. Acta 1186 (1994) 117–122.
[61] C. Rischel, D. Spiedel, J.P. Ridge, M.R. Jones, J. Breton, J.-C. Lambry, J.-L. Martin, M.H. Vos, Proc. Natl. Acad. Sci. USA 95 (1998) 12306–12311.
[62] J. Rautter, F. Lendzian, C. Schulz, A. Fetsch, M. Kuhn, X. Lin, J.C. Williams, J.P. Allen, W. Lubitz, Biochemistry 34 (1995) 8130–8143.
[63] R. van Grondelle, J.P. Dekker, T. Gillbro, V. Sundström, Biochim. Biophys. Acta 1187 (1994) 1–65.
[64] R.J. Stanley, B. King, S.G. Boxer, J. Phys. Chem. 100 (1996) 12052–12059.
[65] M.H. Vos, J. Breton, J.-L. Martin, J. Phys. Chem. B 101 (1997) 9820–9832.
[66] R. Jimenez, F. van Mourik, J.Y. Yu, G.R. Fleming, J. Phys. Chem. B 101 (1997) 7350–7359.
[67] U. Liebl, J.-C. Lambry, W. Leibl, J. Breton, J.-L. Martin, M.H. Vos, Biochemistry 35 (1996) 9925–9934.
[68] U. Liebl, J.-C. Lambry, J. Breton, J.-L. Martin, M.H. Vos, Biochemistry 36 (1997) 5912–5920.
[69] M. Du, X. Xie, Y. Jia, L. Mets, G.R. Fleming, Chem. Phys. Lett. 201 (1993) 535–542.
[70] J. Breton, J.-L. Martin, A. Migus, A. Antonetti, A. Orszag, Proc. Natl. Acad. Sci. USA 83 (1986) 5121–5125.
[71] N.W. Woodbury, M. Becker, D. Middendorf, W.W. Parson, Biochemistry 24 (1985) 7516–7521.
[72] C. Kirmaier, D. Holten, FEBS Lett. 239 (1988) 211–218.
[73] G.R. Fleming, J.- Martin L, J. Breton, Nature 333 (1988) 190–192.
[74] W. Zinth, W. Kaiser, in: J. Deisenhofer, J.R. Norris (Eds.), The Photosynthetic Reaction Center, vol. II, Academic Press, San Diego, 1993, pp. 71–88.
[75] C. Kirmaier, D. Holten, in: J. Deisenhofer, J.R. Norris (Eds.), The Photosynthetic Reaction Center, vol. II, Academic Press, San Diego, 1993, pp. 49–70.
[76] N.W. Woodbury, J.P. Allen, in: R.E. Blankenship, M.T. Madigan, C.E. Bauer (Eds.), Anoxygenic Photosynthetic Bacteria, Kluwer, Dordrecht, 1995, pp. 527–557.
[77] S. Franzen, J.-L. Martin, Annu. Rev. Phys. Chem. 46 (1995) 453–487.
[78] A.J. Hoff, J. Deisenhofer, Phys. Rep. 287 (1997) 1–247.
[79] R.A. Marcus, N. Sutin, Biochim. Biophys. Acta 811 (1985) 265–322.
[80] C.C. Moser, J.M. Keske, K. Warncke, R.S. Farid, P.L. Dutton, Nature 355 (1992) 796–802.
[81] R.A. Marcus, Chem. Phys. Lett. 133 (1987) 471–477.
[82] M. Bixon, J. Jortner, M.E. Michel-Beyerle, Biochim. Biophys. Acta 1056 (1991) 301–315.
[83] W. Holzapfel, U. Finkele, W. Kaiser, D. Oesterhelt, H. Scheer, H.U. Stilz, W. Zinth, Chem. Phys. Lett. 160 (1989) 1–7.

[84] W. Holzapfel, U. Finkele, W. Kaiser, D. Oesterhelt, H. Scheer, H.U. Stilz, W. Zinth, Proc. Natl. Acad. Sci. USA 87 (1990) 5168–5172.
[85] S. Schmidt, T. Arlt, P. Hamm, H. Huber, T. Nägele, J. Wachtveitl, W. Zinth, M. Meyer, H. Scheer, Spectrochim. Acta A 51 (1995) 1565–1578.
[86] A.R. Holzwarth, M.G. Müller, Biochemistry 35 (1996) 11820–11831.
[87] C.-K. Chan, T.J. DiMagno, L.X.Q. Chen, J.R. Norris, G.R. Fleming, Proc. Natl. Acad. Sci. USA 88 (1991) 11202–11206.
[88] C. Lauterwasser, U. Finkele, H. Scheer, W. Zinth, Chem. Phys. Lett. 183 (1991) 471–477.
[89] M.H. Vos, J.-C. Lambry, S.J. Robles, D.C. Youvan, J. Breton, J.-L. Martin, Proc. Natl. Acad. Sci. USA 89 (1992) 613–617.
[90] S. Spörlein, W. Zinth, J. Wachtveitl, J. Phys. Chem. B 102 (1998) 7492–7496.
[91] D.M. Jonas, M.J. Lang, Y. Nagasawa, T. Joo, G.R. Fleming, J. Phys. Chem. 100 (1996) 12660–12673.
[92] G. Haran, K. Wynne, C.C. Moser, P. Dutton L, R.M. Hochstrasser, J. Phys. Chem. 100 (1996) 5562–5569.
[93] M.-L. Groot, J.-Y. Yu, R. Agarwal, J.R. Norris, G.R. Fleming, J. Phys. Chem. B 102 (1998) 5923–5931.
[94] M.E. van Brederode, M.R. Jones, R. van Grondelle, Chem. Phys. Lett. 268 (1997) 143–149.
[95] M.E. van Brederode, M.R. Jones, F. van Mourik, I.H.M. van Stokkum, R. van Grondelle, Biochemistry 36 (1997) 6855–6861.
[96] S. Lin, A.K.W. Taguchi, N.W. Woodbury, J. Phys. Chem. 100 (1996) 17067–17078.
[97] M.E. van Brederode, F. van Mourik, I.H.M. van Stokkum, M.R. Jones, R. van Grondellle, XIth International Congress on Photosynthesis, 1998, SY4-P115.
[98] S. Lin, J. Jackson, A.K.W. Taguchi, N.W. Woodbury, J. Phys. Chem. B 102 (1998) 4016–4022.
[99] J.A. Jackson, S. Lin, A.K.W. Taguchi, J.C. Williams, J.P. Allen, N.W. Woodbury, J. Phys. Chem. B 101 (1997) 5747–5754.
[100] S.A.P. Merry, S. Kumazaki, Y. Tachibana, D.M. Joseph, G. Porter, K. Yoshihara, J. Barber, J.R. Durrant, D.R. Klug, J. Phys. Chem. 100 (1996) 10469–10478.
[101] J. Koepke, H. Xiche, C. Muenke, K. Schulten, H. Michel, Structure 4 (1996) 581–597.
[102] S. Karrasch, P.A. Bullough, R. Ghosh, EMBO J. 14 (1995) 631–638.
[103] A.P. Shreve, J.K. Trautmann, H.A. Frank, T.G. Owens, A.C. Albrecht, Biochim. Biophys. Acta 1058 (1991) 280–288.
[104] V. Nagarajan, R.G. Alden, J.C. Williams, W.W. Parson, Proc. Natl. Acad. Sci. USA 93 (1996) 13774–13779.
[105] T. Pullerits, M. Chachisvilis, V. Sundström, J. Phys. Chem. 100 (1996) 10787–10792.
[106] V.I. Novoderezkin, A.P. Razjivin, FEBS Lett. 368 (1995) 370–372.
[107] J.M. Kennis, A.M. Streltsov, T.J. Aartsma, T. Nozawa, J. Amesz, J. Phys. Chem. B 101 (1997) 7350–7359.
[108] D. Leupold, H. Stiel, K. Teuchner, F. Nowak, W. Sandner, B. Ücker, H. Scheer, Phys. Rev. Lett. 77 (1996) 4675–4678.
[109] R. Monshouwer, A. Baltuska, F. van Mourik, R. van Grondelle, J. Phys. Chem. A 102 (1998) 4360–4371.
[110] T. Meier, V. Chernyak, S. Mukamel, J. Phys. Chem. B 101 (1997) 7332–7342.
[111] V. Nagarajan, E. Johnson, J.C. Williams, W.W. Parson, J. Phys. Chem. (1999) in press.
[112] J. Nathans, Biochemistry 31 (1992) 4923–4931.
[113] R.A. Mathies, S.W. Lin, J.B. Ames, W.T. Pollard, Annu. Rev. Biochem. Bioeng. 20 (1991) 491–518.
[114] J.W. Petrich, J. Breton, J.-L. Martin, A. Antonetti, Chem. Phys. Lett. 137 (1987) 369–375.
[115] R.A. Mathies, C.H. Brito Cruz, W.T. Pollard, C.W. Shank, Science 240 (1988) 777–779.
[116] J. Dobler, W. Zinth, W. Kaiser, D. Oesterhelt, Chem. Phys. Lett. 144 (1988) 215–220.
[117] W.T. Pollard, S.-Y. Lee, R.A. Mathies, J. Chem. Phys. 92 (1990) 4012–4029.
[118] M. Du, G.R. Fleming, Biophys. Chem. 48 (1993) 101–111.
[119] K.C. Hasson, F. Gai, P.A. Anfinrud, Proc. Natl. Acad. Sci. USA 93 (1996) 15124–15129.
[120] F. Gai, K.C. Hasson, J. Cooper McDonald, P.A. Anfinrud, Science 279 (1998) 1886–1891.
[121] G. Haran, K. Wynne, A. Xie, Q. He, M. Chance, R.M. Hochstrasser, Chem. Phys. Lett. 261 (1996) 389–395.
[122] K. Schulten, W. Humphrey, I. Logunov, M. Sheves, D. Xu, Israel J. Chem. 35 (1995) 447–464.
[123] S.L. Shapiro, A.J. Campillo, A. Lewis, G.J. Perreault, J.P. Spoonhower, R.J. Clayton, W. Stoeckenius, Biophys. J. 23 (1978) 383–393.
[124] S.L. Logunov, T.M. Masciangioli, V.F. Kamalov, M.A. El-Sayed, J. Phys. Chem. B 102 (1998) 2303–2306.
[125] L. Song, M.A. El-Sayed, J.K. Lanyi, Science 261 (1993) 891–894.
[126] L. Song, M.A. El-Sayed, J.K. Lanyi, J. Phys. Chem. 100 (1996) 10479–10481.
[127] S.L. Logunov, M.A. El-Sayed, L. Song, J.K. Lanyi, J. Phys. Chem. 100 (1996) 2391–2398.
[128] Y. Schichida, Photochem. Photobiol. 52 (1990) 1179–1185.
[129] M. Yan, D. Manor, G. Weng, H. Chao, L. Rothberg, T.M. Jedju, R.R. Alfano, R.H. Callender, Proc. Natl. Acad. Sci. USA 88 (1991) 9809–9812.
[130] R.W. Schoenlein, L.A. Peteanu, R.A. Mathies, C.V. Shank, Science 254 (1991) 412–415.
[131] L.A. Peteanu, R.W. Schoenlein, Q. Wang, R.A. Mathies, C.V. Shank, Proc. Natl. Acad. Sci. USA 90 (1993) 11762–11766.
[132] Q. Wang, R.W. Schoenlein, L.A. Peteanu, R.A. Mathies, C.V. Shank, Science 266 (1994) 422–424.
[133] R.W. Schoenlein, L.A. Peteanu, Q. Wang, R.A. Mathies, C.V. Shank, J. Phys. Chem. 97 (1993) 12087–12092.

[134] Q. Wang, G.G. Kochendoerfer, R.W. Schoenlein, P.J.E. Verdegem, J. Lugtenburg, R.A. Mathies, C.V. Shank, J. Phys. Chem. 100 (1996) 17388–17394.
[135] J.-L. Martin, A. Migus, C. Poyart, Y. Lecarpentier, R. Astier, A. Antonetti, Proc. Natl. Acad. Sci. USA 80 (1983) 173–177.
[136] J.-L. Martin, M.H. Vos, Methods Enzymol. 232 (1994) 416–430.
[137] J.W. Petrich, C. Poyart, J.-L. Martin, Biochemistry 27 (1988) 4049–4060.
[138] P.O. Stoutland, J.-C. Lambry, J.-L. Martin, W.H. Woodruff, J. Phys. Chem. 95 (1991) 6406–6408.
[139] J.W. Petrich, J.-C. Lambry, K. Kuczera, M. Karplus, C. Poyart, J.-L. Martin, Biochemistry 30 (1991) 3975–3987.
[140] K.N. Walda, X.Y. Liu, V.S. Sharma, D. Magde, Biochemistry 33 (1994) 2198–2209.
[141] J.W. Petrich, J.-C. Lambry, S. Balasubramian, D.G. Lambright, S.G. Boxer, J.-L. Martin, J. Mol. Biol. 238 (1994) 437–444.
[142] M.L. Carlson, R. Regan, R. Elber, H. Li, G.N. Phillips, J.S. Olson, Q.H. Gibson, Biochemistry 33 (1994) 10597–10606.
[143] V. Srajer, P.M. Champion, Biochemistry 30 (1991) 7390–7402.
[144] X.-Y. Li, M.Z. Zgierski, Chem. Phys. Lett. 188 (1992) 16–20.
[145] S. Franzen, B. Bohn, C. Poyart, J.-L. Martin, Biochemistry 34 (1995) 1224–1237.
[146] M. Lim, T.A. Jackson, P.A. Anfinrud, Proc. Natl. Acad. Sci. USA 90 (1993) 5801–5804.
[147] K. Kuczera, J.-C. Lambry, J.-L. Martin, M. Karplus, Proc. Natl. Acad. Sci. USA 90 (1993) 5805–5807.
[148] L. Zhu, J.T. Sage, P.M. Champion, Science 266 (1994) 629–632.
[149] S.A. Asher, Methods Enzymol. 76 (1981) 371–413.
[150] M. Lim, T.A. Jackson, P.A. Anfinrud, Nat. Struct. Biol. 4 (1997) 209–214.
[151] J.R. Lingle, X. Xu, H. Zhu, S.-C. Yu, J.B. Hopkins, J. Phys. Chem. 95 (1991) 9320–9331.
[152] T. Lian, B. Locke, Y. Kholodenko, R.M. Hochstrasser, J. Phys. Chem. 98 (1994) 11648–11656.
[153] J.R. Hill, A. Tokmakoff, K.A. Peterson, B. Sauter, D. Zimdars, D.D. Dlott, M.D. Fayer, J. Phys. Chem. 98 (1994) 11213–11219.
[154] J.R. Hill, D.D. Dlott, C.W. Rella, K.A. Peterson, S.M. Decatur, S.G. Boxer, M.D. Fayer, J. Phys. Chem. 100 (1996) 12100–12107.
[155] K.D. Rector, C.W. Rella, J.R. Hill, A.S. Kwok, S.G. Sligar, E.Y.T. Chien, D.D. Dlott, M.D. Fayer, J. Phys. Chem. B 101 (1997) 1468–1475.
[156] K.D. Rector, J.R. Engholm, J.R. Hill, D.J. Myers, R. Hu, S.G. Boxer, D.D. Dlott, M.D. Fayer, J. Phys. Chem. B 102 (1998) 331–333.
[157] S. Yoshikawa, K. Shinzawa-Itoh, R. Nakashima, R. Yaono, E. Yamashita, N. Inoue, M. Yao, M.J. Fei, C. Peters Libeu, T. Mizushima, H. Yamaguchi, T. Tomizaki, T. Tsukihara, Science 280 (1998) 1723–1729.
[158] Ó. Einarsdottir, Biochim. Biophys. Acta 1229 (1995) 129–147.
[159] R.B. Dyer, K.A. Peterson, P.O. Stoutland, W.H. Woodruff, J. Am. Chem. Soc. 113 (1991) 6276–6277.
[160] R.B. Dyer, K.A. Peterson, P.O. Stoutland, W.H. Woodruff, Biochemistry 33 (1994) 500–507.
[161] W.H. Woodruff, J. Bioenerg. Biomem. 25 (1993) 177–188.
[162] J.P.M. Schelvis, G. Deinum, C.A. Varotsis, S. Ferguson-Miller, G.T. Babcock, J. Am. Chem. Soc. 119 (1997) 8409–8416.
[163] M. Chattoraj, B.A. King, G.U. Bublitz, S.G. Boxer, Proc. Natl. Acad. Sci. USA 93 (1996) 8362–8367.
[164] R.M. Wachter, B.A. King, R. Heim, K. Kallio, R.M. Tsien, S.G. Boxer, S.J. Remington, Biochemistry 36 (1997) 9759–9765.
[165] A.D. Kummer, C. Kompa, H. Lossau, F. Pöllinger-Dammer, M.E. Michel-Beyerle, C.M. Silva, E.J. Bylina, W.J. Coleman, M.M. Yang, D.C. Youvan, Chem. Phys. 237 (1998) 183–193.
[166] H. Kandori, K. Yoshihara, S. Tokutomi, J. Am. Chem. Soc. 114 (1992) 10958–10959.
[167] M. Bischoff, G. Hermann, S. Rentsch, D. Strehlow, J. Phys. Chem. A 102 (1998) 4399–4404.
[168] D. Thorn Leeson, D.A. Wiersma, Nat. Struct. Biol. 2 (1995) 848–851.
[169] D. Thorn Leeson, D.A. Wiersma, Phys. Rev. Lett. 74 (1995) 2138–2141.
[170] D. Thorn Leeson, D.A. Wiersma, K. Fritsch, J. Friedrich, J. Phys. Chem. B 101 (1997) 6331–6340.
[171] P. Hamm, M. Lim, R.M. Hochstrasser, J. Phys. Chem. B 102 (1998) 6123–6138.
[172] M.H. Keyes, M. Falley, R.J. Lumrey, J. Am. Chem. Soc. 93 (1971) 2035.
[173] A.P. Shreve, N.J. Cherepy, S. Franzen, S.G. Boxer, R.A. Mathies, Proc. Natl. Acad. Sci. USA 88 (1991) 11207–11211.
[174] K. Czarnecki, J.R. Diers, V. Chynwat, J.P. Erickson, H.A. Frank, D.F. Bocian, J. Am. Chem. Soc. 119 (1997) 415–426.

The process begins with the protein reconstituted into the curved bilayer of the `bicontinuous' cubic phase (tan). Added `precipitants' shift the equilibrium away from stability in the cubic membrane.Â Serial femtosecond X-ray crystallography (SFX) is a relatively new method for collecting crystallographic information from small crystals fed into a free-electron laser (FEL) beam composed of high-fluence X-ray bunches mere femtoseconds long (Chapman et al., 2011 , 2014 ; Spence et al., 2012). Each encounter between an X-ray bunch and a microcrystal (hit) ideally gives rise to a single, still diffraction pattern with greater than ten measurable reflections. Primary process of phytochrome â€“ initial step of photomorphogenesis in green plants. J Am Chem Soc. 1992;114:10958â€“9.Google Scholar. Kennis JTM, et al. Uncovering the hidden ground state of green fluorescent protein. Proc Natl Acad Sci USA. 2004;101:17988â€“93.PubMedGoogle Scholar. Kukura P, McCamant DW, Yoon S, Wandschneider DB, Mathies RA.Â Femtosecond stimulated Raman study of excited-state evolution in bacteriorhodopsin. J Phys Chem B. 2005;109:10449â€“57.PubMedCentralPubMedGoogle Scholar. McCusker JK.Â Renger T, Schlodder E. Primary photophysical processes in photosystem II: bridging the gap between crystal structure and optical spectra. Chemphyschem. 2010;11:1141â€“53.PubMedGoogle Scholar.